Supporting Information

Pressure-Dependent Optoelectronic Properties of Antiperovskite Derivatives X_3AsCl_3 (X = Mg, Ca, Sr, Ba): A First-Principles Study

Tao Hu[1#], Changhe Wu[1#], Mingjun Li[1], Xin Luo[1], Yihao Hou[1], Shichang Li[1, 2], Shengnan Duan[1], Dengfeng Li[1, 2, a)], Gang Tang[3, a)], and Chunbao Feng[1, 2, a)]

AFFILIATIONS
[1]*School of Science, Chongqing University of Posts and Telecommunications, Chongqing 400065, China*
[2]*Institute for Advanced Sciences, Chongqing University of Posts and Telecommunications, Chongqing 400065, China*
[3]*Advanced Research Institute of Multidisciplinary Science, Beijing Institute of Technology, Beijing 100081, China*

[a)]Correspondence and requests for materials should be addressed to: lidf@cqupt.edu.cn (D. L.), gtang@bit.edu.cn (G. T.) and fengcb@cqupt.edu.cn (C. B. F)

[#]These authors contributed equally.

Mechanical properties

The elastic constants were calculated using VASP with the settings IBRION = 6, ISIF = 3, and NFREE = 2. The elastic tensor (C_{ij}) is determined by performing six finite distortions of the lattice and deriving the elastic constants from the strain-stress relationship.[1]

Based on the calculated C_{ij}, the mechanical properties, including the bulk modulus (B), shear modulus (G), and Young's modulus (Y), were determined using the Voigt-Reuss-Hill (VRH) approximation[2, 3]. For the cubic structure, considering its crystal symmetries, the values of B, G, and Y are calculated as follows: [4, 5]

$$B = \frac{C_{11} + 2C_{12}}{3} \quad (1)$$

$$G = \frac{C_{11} - C_{12} + 3C_{44}}{5} \quad (2)$$

$$Y = \frac{9BG}{3B + G} \quad (3)$$

As shown in Table S2, both the C_{ij} values and the mechanical moduli follow the trend $Mg_3AsCl_3 > Ca_3AsCl_3 > Sr_3AsCl_3 > Ba_3AsCl_3$. This trend is attributed to the increasing ionic radii of the divalent cations: $r(Mg^{2+}) < r(Ca^{2+}) < r(Sr^{2+}) < r(Ba^{2+})$. Larger ionic radii lead to longer bond lengths, resulting in lower C_{ij} values and mechanical moduli. Since hydrostatic pressure reduces bond lengths, the C_{ij} values and mechanical moduli for all four compounds increase with increasing pressure. Moreover, X_3AsCl_3 (X^{2+} = Mg, Ca, Sr, Ba) exhibit Young's moduli ranging from 39 to 81 GPa at 0 GPa, which are higher than those of organic-inorganic hybrid halide perovskites (17 - 22 GPa),[5] but significantly lower than those of inorganic antiperovskites (90 - 182 GPa).[6]

Murnaghan EOS equation

The Murnaghan EOS model assumes that the bulk modulus varies linearly with pressure. The resulting energy-volume relationship is given as:[7]

$$E(v) = E_0 + \frac{BV_0}{B' + 1}\left(\frac{v^{-B'} - 1}{B'} + v - 1\right) \quad (4)$$

where $v = \frac{V}{V_0}$, V_0 and E_0 are the volume and energy at zero pressure respectively. B and B' are the values of modules and its pressure derivative respectively. B_0 and B_0' represent the bulk modulus and its pressure derivative at 0 GPa and can be determined by setting $v = 1$ in the above equation.

Optical properties

The optical absorption spectra of Mg_3AsCl_3, Ca_3AsCl_3, Sr_3AsCl_3 and Ba_3AsCl_3 are described by the complex dielectric function, i.e. $\varepsilon(\omega) = \varepsilon_1(\omega) + i\varepsilon_2(\omega)$. Based on the dielectric function of investigated systems, the absorption coefficient $\alpha(\omega)$ can be given by the following equation:

$$\alpha(\omega) = \frac{\sqrt{2}\omega}{c}\left(\sqrt{\varepsilon_1^2 - \varepsilon_2^2} - \varepsilon_1\right)^{\frac{1}{2}} \quad (5)$$

where $\varepsilon_1(\omega)$ is the real part of the dielectric function, $\varepsilon_2(\omega)$ is the imaginary part, and ω is the optical frequency.[8]

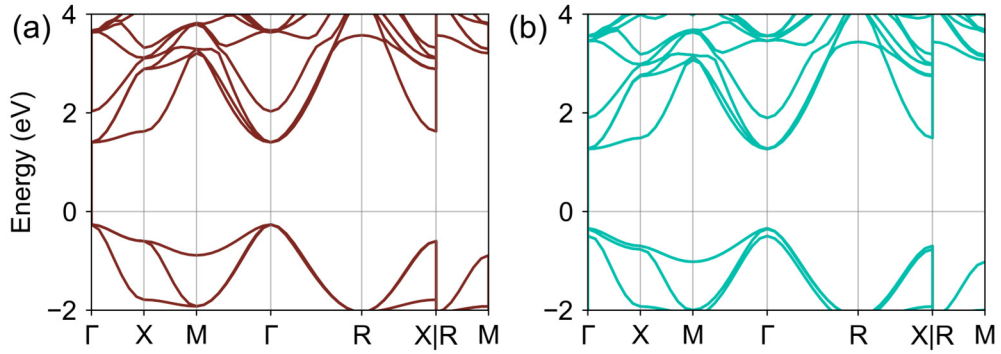

Figure S1. Band structure of Ba_3AsCl_3 calculated using (a) HSE06 and (b) HSE06+SOC.

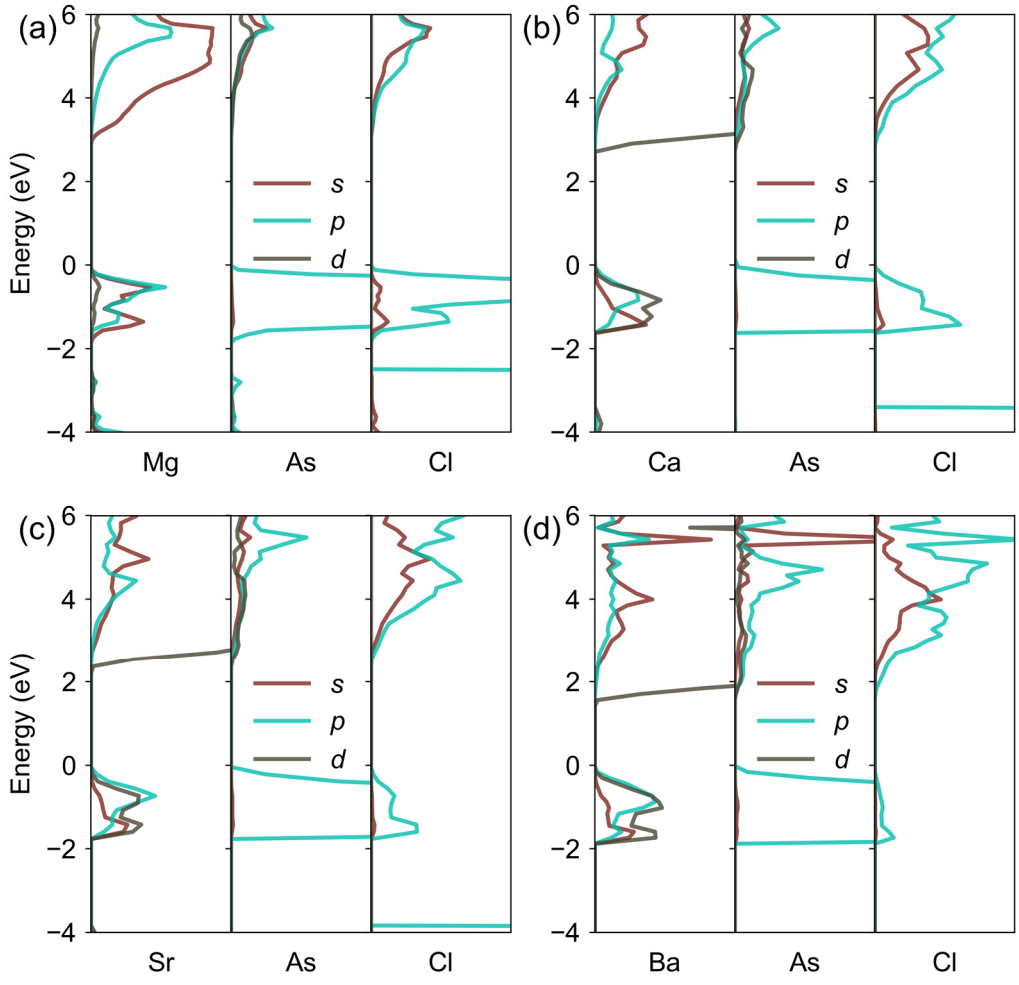

Figure S2. PDOS for (a) Mg_3AsCl_3, (b) Ca_3AsCl_3, (c) Sr_3AsCl_3, and (d) Ba_3AsCl_3.

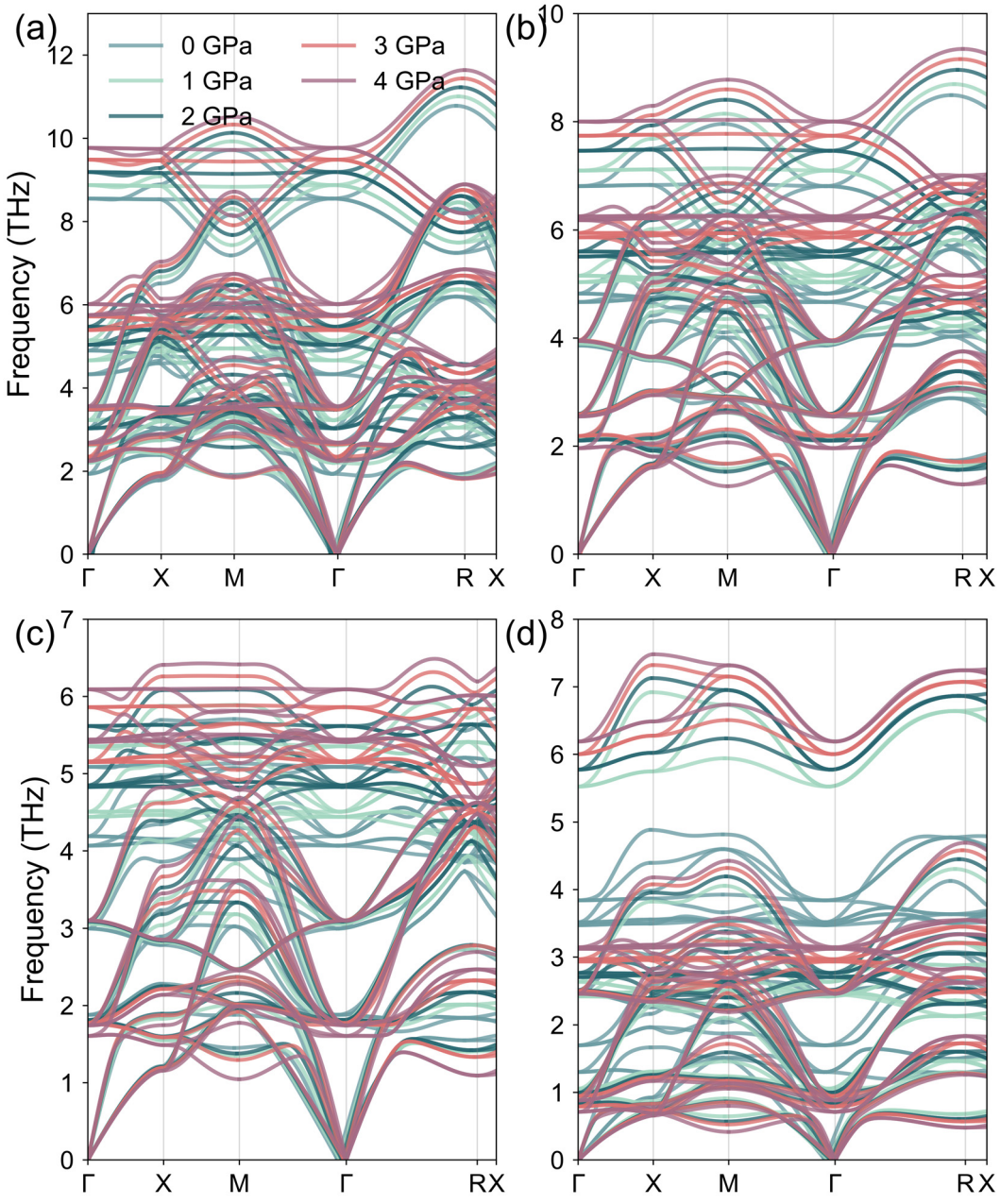

Figure S3. Phonon spectra under pressure for (a) Mg_3AsCl_3, (b) Ca_3AsCl_3, (c) Sr_3AsCl_3, and (d) Ba_3AsCl_3.

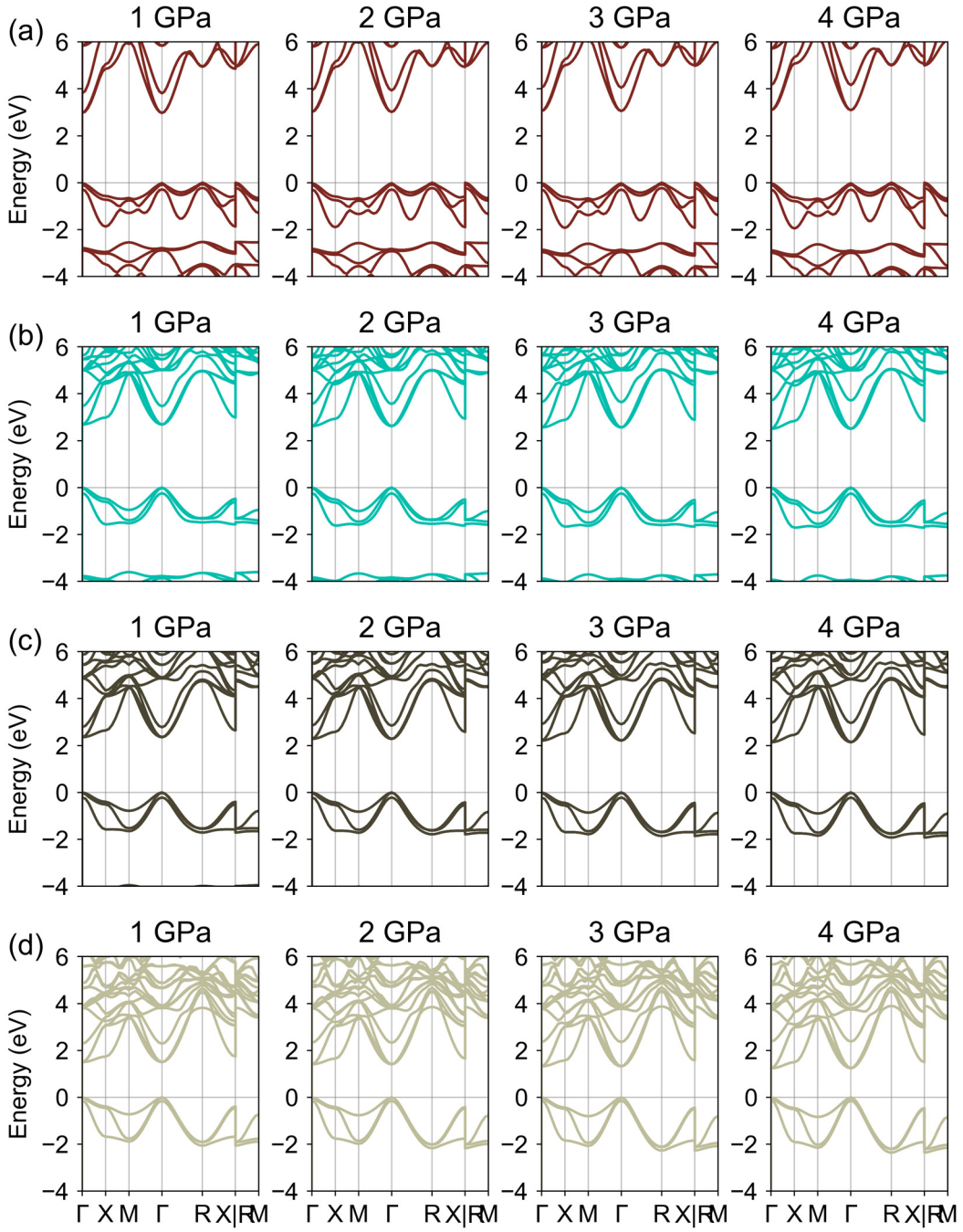

Figure S4. Band structure (aligned to the VBM) under pressures of 1 to 4 GPa, calculated with HSE06+SOC for (a) Mg_3AsCl_3, (b) Ca_3AsCl_3, (c) Sr_3AsCl_3, and (d) Ba_3AsCl_3.

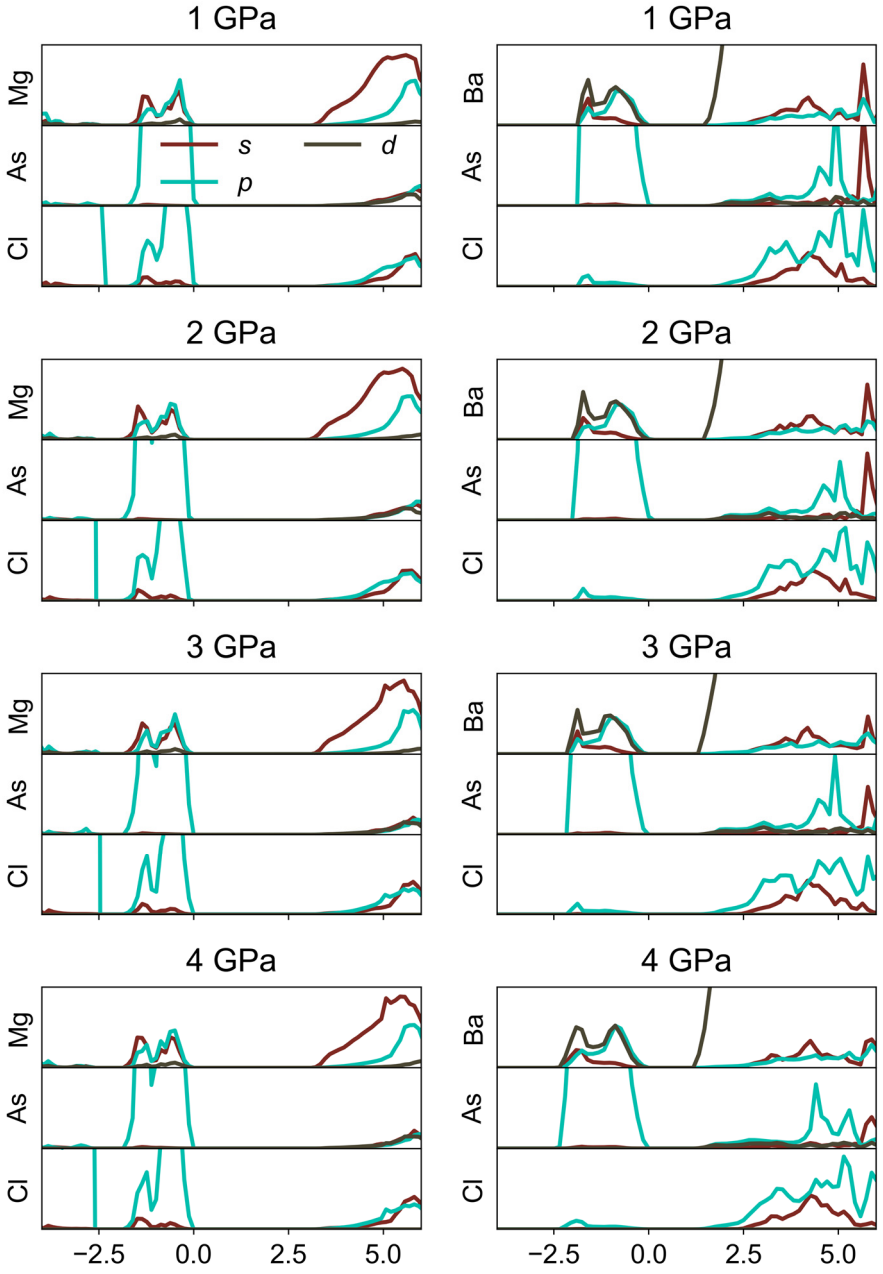

Figure S5. Projected density of states (PDOS) of Mg_3AsCl_3 (left panel) and Ba_3AsCl_3 (right panel) under pressures from 1 GPa to 4 GPa.

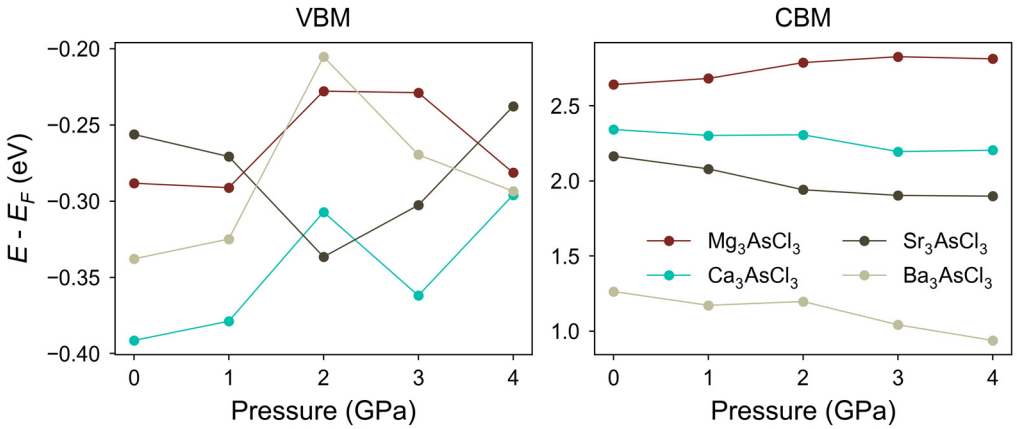

Figure S6. Changes in the VBM and CBM for Mg_3AsCl_3, Ca_3AsCl_3, Sr_3AsCl_3, and Ba_3AsCl_3 under pressures ranging from 1 GPa to 4 GPa.

Table S1. The ionic (ε_{ion}) and electronic (ε_{∞}) contributions to the static dielectric constant (ε_{st}) for X_3AsCl_3 (X=Mg, Ca, Sr, Ba) under different pressure.

Compound	Pressure (GPa)	ε^{xx}_{ion}	ε^{yy}_{ion}	ε^{zz}_{ion}	$\varepsilon^{xx}_{\infty}$	$\varepsilon^{yy}_{\infty}$	$\varepsilon^{zz}_{\infty}$	ε^{xx}_{st}	ε^{yy}_{st}	ε^{zz}_{st}
Mg_3AsCl_3	0	18.294	18.294	18.294	4.665	4.665	4.665	22.959	22.959	22.959
	1	15.137	15.137	15.137	4.652	4.652	4.652	19.789	19.789	19.789
	2	12.694	12.694	12.694	4.643	4.643	4.643	17.337	17.337	17.337
	3	11.248	11.248	11.248	4.630	4.630	4.630	15.878	15.878	15.878
	4	10.114	10.114	10.114	4.627	4.627	4.627	14.741	14.741	14.741
Ca_3AsCl_3	0	6.877	6.877	6.877	4.462	4.462	4.462	11.339	11.339	11.339
	1	6.166	6.166	6.166	4.521	4.521	4.521	10.687	10.687	10.687
	2	5.573	5.573	5.573	4.600	4.600	4.600	10.173	10.173	10.173
	3	5.271	5.271	5.271	4.671	4.671	4.671	9.942	9.942	9.942
	4	5.027	5.027	5.027	4.744	4.744	4.744	9.771	9.771	9.771
Sr_3AsCl_3	0	6.265	6.265	6.265	4.254	4.254	4.254	10.519	10.519	10.519
	1	5.657	5.657	5.657	4.329	4.329	4.329	9.986	9.986	9.986
	2	5.241	5.241	5.241	4.411	4.411	4.411	9.652	9.652	9.652
	3	4.975	4.975	4.975	4.499	4.499	4.499	9.474	9.474	9.474
	4	4.809	4.809	4.809	4.593	4.593	4.593	9.402	9.402	9.402
Ba_3AsCl_3	0	8.624	8.624	8.624	4.930	4.930	4.930	13.554	13.554	13.554
	1	7.835	7.835	7.835	5.231	5.231	5.231	13.066	13.066	13.066
	2	7.633	7.633	7.633	5.585	5.585	5.585	13.218	13.218	13.218
	3	7.809	7.809	7.809	6.043	6.043	6.043	13.852	13.852	13.852
	4	7.563	7.563	7.563	6.172	6.172	6.172	13.735	13.735	13.735

Table S2. The elastic constants (C_{ij}), bulk modulus (B) shear modulus (G) and Young's modulus (Y), for X_3AsCl_3 (X=Mg, Ca, Sr, Ba) under different pressure.

Compound	Pressure (GPa)	C_{ij} (GPa)			B_{VRH} (GPa)	G_{VRH} (GPa)	Y_{VRH} (GPa)
		C_{11}	C_{12}	C_{44}			
Mg_3AsCl_3	0	95.478	27.159	31.726	49.932	32.678	80.477
	1	102.609	27.563	32.326	52.578	34.314	84.548
	2	110.198	28.272	32.904	55.581	35.921	88.662
	3	117.860	28.995	33.099	58.616	37.246	92.209
	4	125.381	29.661	33.760	61.568	38.835	96.265
Ca_3AsCl_3	0	85.882	13.256	19.572	37.465	25.133	61.620
	1	94.088	13.358	19.731	40.268	26.393	64.983
	2	104.669	13.409	19.808	43.829	27.870	68.988
	3	113.504	13.416	19.888	46.779	29.078	72.260
	4	122.388	13.422	19.737	49.744	30.066	75.072
Sr_3AsCl_3	0	75.869	9.995	15.141	31.953	20.788	51.249
	1	85.108	10.092	15.053	35.098	21.914	54.416
	2	94.592	10.085	14.904	38.254	22.977	57.432
	3	103.893	10.069	14.714	41.344	23.937	60.195
	4	113.102	10.006	14.489	44.371	24.825	62.768
Ba_3AsCl_3	0	63.166	8.343	10.938	26.617	15.964	39.912
	1	74.077	8.362	10.620	30.267	17.039	43.040
	2	83.993	8.484	10.044	33.653	17.673	45.121
	3	93.294	8.359	9.550	36.670	18.280	47.025

Table S3. Lattice constants, HSE06+SOC Band gap (E_g, with I for indirect and D for direct bandgap), ionic (ε_{ion}) and electronic (ε_{∞}) dielectric constant, average effective mass of hole (m_h^*) and electron (m_e^*), Exciton Binding Energy (E_b), and Spectroscopic Limited Maximum Efficiency (SLME) at 2 μm film thickness for Mg_3AsCl_3, Ca_3AsCl_3, Sr_3AsCl_3, and Ba_3AsCl_3 under varying pressures.

Compounds	Pressure (GPa)	a (Å)	E_g (eV)	ε_{ion}	ε_{∞}	m_h^* (m_0)	m_e^* (m_0)	E_b (eV)	SLME (%)
Mg_3AsCl_3	0	5.32, 5.32[9]	2.93 (I), 3.00[9]	18.294	4.665	0.388	0.375	0.119	4.77
	1	5.288	2.97 (I)	15.137	4.652	0.383	0.372	0.118	4.18
	2	5.256	3.01(I)	12.694	4.643	0.380	0.370	0.118	3.68
	3	5.227	3.06(I)	11.248	4.630	0.376	0.367	0.117	3.22
	4	5.200	3.09 (I)	10.114	4.627	0.373	0.366	0.117	3.01
Ca_3AsCl_3	0	5.79, 5.80[9]	2.73 (D), 2.84[9]	6.877	4.462	0.389	0.539	0.154	7.89
	1	5.743	2.68 (D)	6.166	4.521	0.378	0.506	0.144	8.72
	2	5.692	2.61 (D)	5.573	4.600	0.366	0.482	0.133	9.95
	3	5.652	2.56 (D)	5.271	4.671	0.356	0.463	0.125	10.97
	4	5.615	2.50(D)	5.027	4.744	0.345	0.446	0.117	12.01
Sr_3AsCl_3	0	6.12, 6.12[9]	2.42 (D), 2.47[9]	6.265	4.254	0.398	0.524	0.169	13.62
	1	6.064	2.35 (D)	5.657	4.329	0.384	0.504	0.158	15.02
	2	6.011	2.28(D)	5.241	4.411	0.370	0.483	0.146	16.40
	3	5.963	2.21(D)	4.975	4.499	0.357	0.464	0.135	17.83
	4	5.919	2.14(D)	4.809	4.593	0.345	0.445	0.125	19.31
Ba_3AsCl_3	0	6.51, 6.51[9]	1.60 (D), 1.62[9]	8.624	4.930	0.363	0.522	0.119	29.58

	1	6.429	1.50 (D)	7.835	5.231	0.341	0.482	0.099	31.14
	2	6.363	1.40 (D)	7.633	5.585	0.321	0.453	0.082	32.29
	3	6.306	1.31 (D)	7.809	6.043	0.303	0.426	0.066	32.41
	4	6.259	1.23 (D)	7.563	6.172	0.288	0.403	0.060	31.94

Table S4. Band index and corresponding Mulliken symbols and Koster notation for O_h and D_{4h} point groups.

K		Γ (0.0 0.0 0.0)			X (0.0 0.5 0.0)			M (0.5 0.5 0.0)			R (0.5 0.5 0.5)		
Symmetry		O_h			D_{4h}			D_{4h}			O_h		
		Band Index	Mulliken Symbol	Koster Notation	Band Index	Mulliken Symbol	Koster Notation	Band Index	Mulliken Symbol	Koster Notation	Band Index	Mulliken Symbol	Koster Notation
Mg_3AsCl_3	CBM	3	E_g	Γ_3^+	9	B_{2u}	X_4^-	1	A_{1g}	M_1^+	9	T_{1u}	R_4^-
	VBM	9	T_{1u}	Γ_4^-	5	E_g	X_5^+	10	E_u	M_5^-	5	T_{2g}	R_5^+
Ca_3AsCl_3	CBM	5	T_{2g}	Γ_5^+	8	B_{1u}	X_3^-	7	A_{2u}	M_2^-	9	T_{1u}	R_4^-
	VBM	9	T_{1u}	Γ_4^-	5	E_g	X_5^+	8	B_{1u}	M_3^-	5	T_{2g}	R_5^+
Sr_3AsCl_3	CBM	5	T_{2g}	Γ_5^+	8	B_{1u}	X_3^-	7	A_{2u}	M_2^-	9	T_{1u}	R_4^-
	VBM	9	T_{1u}	Γ_4^-	5	E_g	X_5^+	8	B_{1u}	M_3^-	5	T_{2g}	R_5^+
Ba_3AsCl_3	CBM	5	T_{2g}	Γ_5^+	8	B_{1u}	X_3^-	7	A_{2u}	M_2^-	1	A_{1g}	R_1^+
	VBM	9	T_{1u}	Γ_4^-	5	E_g	X_5^+	8	B_{1u}	M_3^-	5	T_{2g}	R_5^+

REFERENCES

1. Y. Le Page and P. Saxe, *Physical Review B*, 2002, **65**, 104104.
2. Z.-j. Wu, E.-j. Zhao, H.-p. Xiang, X.-f. Hao, X.-j. Liu and J. Meng, *Physical Review B*, 2007, **76**, 054115.
3. R. Hill, *Proceedings of the Physical Society. Section A*, 1952, **65**, 349.
4. P. Ravindran, L. Fast, P. A. Korzhavyi, B. Johansson, J. Wills and O. Eriksson, *Journal of Applied Physics*, 1998, **84**, 4891–4904.
5. M. Faghihnasiri, M. Izadifard and M. E. Ghazi, *The Journal of Physical Chemistry C*, 2017, **121**, 27059-27070.
6. H. Zhong, C. Feng, H. Wang, D. Han, G. Yu, W. Xiong, Y. Li, M. Yang, G. Tang and S. Yuan, *ACS Applied Materials & Interfaces*, 2021, **13**, 48516-48524.
7. K. Latimer, S. Dwaraknath, K. Mathew, D. Winston and K. A. Persson, *npj Computational Materials*, 2018, **4**, 40.
8. V. Wang, N. Xu, J.-C. Liu, G. Tang and W.-T. Geng, *Computer Physics Communications*, 2021, **267**, 108033.
9. H.-J. Feng and Q. Zhang, *Applied Physics Letters*, 2021, **118**.